1-1-2013

Lini0.5mn1.5o4 spinel cathode using room temperature ionic liquid as electrolyte

Xuan-Wen Gao
University of Wollongong, xg973@uowmail.edu.au

Chuanqi Feng
Hubei University, China, cfeng@uow.edu.au

Shulei Chou
University of Wollongong, shulei@uow.edu.au

Jia-Zhao Wang
University of Wollongong, jiazhao@uow.edu.au

Jia-Zeng Sun
Monash University

See next page for additional authors

Lini0.5mn1.5o4 spinel cathode using room temperature ionic liquid as electrolyte

Abstract

In this study, LiNi0.5Mn1.5O4 (LNMO) nanoparticles were prepared as a 5 V cathode material via a rheological phase method and annealed at different temperatures: 680 ◦C, 750 ◦C, and 820 ◦C. The sample annealed at 750 ◦C shows the best performance. A room temperature ionic liquid (RTIL) containing 1 M lithium bis(trifluoromethanesulfonyl) imide (LiNTf2) in N-butyl-N-methyl-pyrrolidinium bis(trifluoromethanesulfonyl) imide (C4mpyrNTf2) was used as novel electrolyte in conjunction with the LNMO cathodes and their electrochemical properties have been investigated. The results show that the LNMO using RTIL as electrolyte has better coulombic efficiency and comparable discharge capacities to those of the cells assembled with standard liquid electrolyte (1 M LiPF6 in ethylene carbonate/diethyl carbonate). Electrochemical impedance spectroscopy shows that the RTIL is much more stable as the electrolyte for LiNi0.5Mn1.5O4 than the conventional electrolyte.

Keywords

5mn1, spinel, liquid, ionic, 5o4, temperature, lini0, electrolyte, room, cathode

Disciplines

Engineering | Physical Sciences and Mathematics

Publication Details

Gao, X., Feng, C., Chou, S., Wang, J., Sun, J., Forsyth, M., McFarlane, D. & Liu, H. (2013). Lini0.5mn1.5o4 spinel cathode using room temperature ionic liquid as electrolyte. Electrochimica Acta, 101 (July), 151-157.

Authors

Xuan-Wen Gao, Chuanqi Feng, Shulei Chou, Jia-Zhao Wang, Jia-Zeng Sun, Maria Forsyth, Doug McFarlane, and Hua-Kun Liu

$LiNi_{0.5}Mn_{1.5}O_4$ Spinel Cathode Using Room Temperature Ionic Liquid as Electrolyte

Xuan-Wen Gao [a], *Chuan-Qi Feng* [b], *Shu-Lei Chou* [a, e*], *Jia-Zhao Wang* [a, e*], *Jia-Zeng Sun* [c, e], *Maria Forsyth* [d, e], *Douglas R. MacFarlane* [c, e], *Hua-Kun Liu* [a, e]

[a] Institute for Superconducting and Electronic Materials, University of Wollongong, Wollongong, NSW 2522 Australia

[b] College of Chemistry and Chemical Engineering, Hubei University, Wuhan 430062, China

[c] School of Chemistry, Monash University, Clayton, Victoria 3800, Australia

[d] Institute for Technology Research and Innovation, Deakin University, Geelong, Vic 3217 Australia

[e] ARC Centre of Excellence for Electromaterials Science, University of Wollongong, Wollongong, NSW 2522, Australia

[*] Corresponding author: shulei@uow.edu.au and jiazhao@uow.edu.au

Abstract:

In this study, $LiNi_{0.5}Mn_{1.5}O_4$ (LNMO) nanoparticles were prepared as a 5 V cathode material via a rheological phase method and annealed at different temperatures: 680 ºC, 750 ºC, and 820 ºC. The sample annealed at 750 ºC shows the best performance. A room temperature ionic liquid (RTIL) containing 1 M lithium bis(trifluoromethanesulfonyl) imide ($LiNTf_2$) in N-butyl-N-methyl-pyrrolidinium bis(trifluoromethanesulfonyl) imide ($C_4mpyrNTf_2$) was used as novel electrolyte in conjunction with the LNMO cathodes and their electrochemical properties have been investigated. The results show that the LNMO using RTIL as electrolyte has better coulombic efficiency and comparable discharge capacities to those of the cells assembled with standard liquid electrolyte (1 M $LiPF_6$ in ethylene carbonate/ diethyl carbonate). Electrochemical impedance spectroscopy shows that the RTIL is much more stable as the electrolyte for $LiNi_{0.5}Mn_{1.5}O_4$ than the conventional electrolyte.

Keywords: Lithium-ion battery; ionic liquid; $LiNi_{0.5}Mn_{1.5}O_4$ nanoparticles; cathode materials; rheological phase method.

1. Introduction:

The search for cathode materials and electrolytes with high voltage capacity for lithium-ion batteries has been intense in recent years, since the capacity of a lithium-ion battery is normally limited by the cathode material due to the safety concerns. In recent years, $LiNi_{0.5}Mn_{1.5}O_4$ (LNMO) has attracted considerable attention from many research groups in the field of energy storage, owing to its high specific energy of 658 Wh kg^{-1} [1-3], which is much higher than commercially available cathode materials such as $LiCoO_2$ (518 Wh kg^{-1}), $LiMn_2O_4$ (400 Wh kg^{-1}), $LiFePO_4$ (495 Wh kg^{-1}), and $LiCo_{1/3}Ni_{1/3}Mn_{1/3}O_2$ (576 Wh kg^{-1}). The major charge/discharge reactions of $LiNi_{0.5}Mn_{1.5}O_4$ take place, however, at ~ 4.7 V (vs. Li/Li^+), which is beyond the stability potential (~4.5 V) of conventional electrolytes ($LiPF_6$ dissolved in carbonates, such as ethylene carbonate (EC), dimethyl carbonate (DMC)/diethyl carbonate (DEC)) [4]. The use of an unstable electrolyte in the high potential range of LNMO results in low coulombic efficiency, which is a major handicap for the commercial of LNMO. Therefore, it is worthwhile to search for highly stable electrolytes for LNMO to improve the coulombic efficiency.

Since Wilkes and Zaworotko reported on room temperature ionic liquids (RTILs) based on the 1-ethyl-3-methylimidazaolium cation and the tetrafluoroborate anion [5], several research groups have focused their work on the development of RTIL electrolyte for lithium batteries. RTILs have shown potential as safe electrolytes for use in lithium ion battery systems, due to their attractive properties, such as electrochemical stability (4.0-5.7 V), thermal stability, and high ionic conductivity [6-8]. In addition, owing to the high reduction dissolution of the active material into conventional organic electrolytes, RTIL for electrolytes can obviously improve the performance of lithium batteries using certain cathode materials, such as S [9, 10], NiS-Ni_7S_6 [11], V_2O_5 [12], and LiV_3O_8 [13]. Among the various RTILs, electrolytes

based on pyrrolidinium systems combined with a lithium salt can be considered as a good benchmark for ionic liquid-based electrolytes. This is because popular imidazolium salts show a window of stability of ~ 4 V, while pyrrolidinium salts, especially those based on imide anions, can show electrochemical stability as high as 6 V [6]. Meanwhile, it has been reported that lithium bis(trifluromethanesulfonyl) amide ($LiNTf_2$), had a beneficial effect on solid electrolyte interphase (SEI) formation on the lithium electrode surface, which plays a key role in terms of the lifetime and safety characteristics of lithium batteries [14]. In a previous work [15], the ionic liquid lithium bis(trifluoromethanesulfonyl) imide ($LiNTf_2$) in N-butyl-N-methylpyrrolidinium bis(trifluoromethanesulfonyle) imide ($C_4mpyrNTf_2$) exhibited relatively high conductivity and low viscosity with 0.5 mol/kg of $LiNTFf_2$. Furthermore, the $LiNTf_2$-$C_4mpyrNTf_2$ system can allow lithium to be cycled with a high degree of reversibility as well, while uniform lithium deposit morphology over many cycles could be achieved at moderate current densities and cycling efficiencies exceeding 99 % have been obtained [16].

In this study, $LiNi_{0.5}Mn_{1.5}O_4$ was prepared by via a rheological phase method. 1 M $LiNTf_2$ in $C_4mpyrNTf_2$ was used as a new electrolyte for Li/$LiNi_{0.5}Mn_{1.5}O_4$ cells without additives, and the relationship between the electrolyte characteristics and the performance of Li/$LiNi_{0.5}Mn_{1.5}O_4$ cells was studied in detail. The electrochemical performance shows that the $LiNi_{0.5}Mn_{1.5}O_4$ nanoparticles using 1 M $LiNTf_2$ in $C_4mpyrNTf_2$ as electrolyte show comparable capacity to that with conventional electrolyte (1 M $LiPF_6$ in EC: DEC = 1:2 (v/v)), as well as significantly improved coulombic efficiency.

2. Experimental

2.1 Synthesis of $LiNi_{0.5}Mn_{1.5}O_4$

The starting materials were analytically pure LiOH, $Ni(CH_3COO)_2 \cdot 4H_2O$, $Mn(CH_3COO)_2 \cdot 4H_2O$, and citric acid. The LiOH, $Ni(CH_3COO)_2 \cdot 4H_2O$, $Mn(CH_3COO)_2 \cdot 4H_2O$, and citric acid were mechanically mixed in the molar ratio of 1:0.5:1.5:3.6 in an agate mortar. After the mixture was ground homogeneously, an appropriate amount of water was added to the powder to obtain a rheological phase state mixture. The mixture was then heated at 90 °C for 12 h, and a precursor was obtained. After that, the precursor was first sintered at 580 °C for 5 h and then was heated at 680 ºC, 750 ºC, and 820 °C for 8 h in air, respectively.

2.2 Materials characterization

Phase analysis of the $LiNi_{0.5}Mn_{1.5}O_4$ nanoparticles was conducted by X-ray diffraction (XRD; Philips PW1730). The morphology and structure of the $LiNi_{0.5}Mn_{1.5}O_4$ were examined by field emission scanning electron microscopy (FESEM) using a JEOL FESEM-7500 30 kV instrument and the specific surface areas were determined by the Brunauer-Emmett-Teller technique (BET, Quanta Chrome Nova 1000).

2.3 Electrochemical characterizations

To test their electrochemical performance, the $LiNi_{0.5}Mn_{1.5}O_4$ samples were mixed at a rate of 80 wt% active materials with 10 wt% carbon black and 10 wt% polyvinylidene fluoride (PVDF). The slurry was uniformly pasted onto pieces of Al foil with an area of 1 cm^2 and dried in a vacuum at 100 ºC for 24 h. Then, the electrodes were compressed before making the cells. Two kinds of electrolytes were used, including a home-made organic solvent-based electrolyte, consisting of 1 M lithium bis(trifluoromethanesulfonyl) amide ($LiNTf_2$) in N-butyl-N-methyl-pyrrolidinium bis(trifluoromethanesulfonyl) amide ($C_4mpyrNTf_2$), and a conventional organic solvent-based electrolyte consisting of 1 M $LiPF_6$ in a 1:2 (v/v) mixture of ethylene carbonate and diethyl carbonate. The coin-type cells (CR2032) were assembled

with a lithium metal counter electrode in an argon-filled glove box. Galvanostatic charge/discharge cycling was conducted using Land Battery Testers in the potential range of 3.5-5.1 V at a current density of 0.1 C (1 C = 140 mA g^{-1}). Electrochemical impedance spectroscopy (EIS) was conducted using a Biologic VMP-3 electrochemical workstation for different potential and cycling states.

3. Results and Discussion

3.1 Structure and morphologies:

Figure 1 presents the XRD patterns obtained from the LNMO powders. All the samples show diffraction peaks characteristic of the cubic spinel structure (space group = Fd3m, JCPDS #32-0581). For the sample annealed at 820 °C, very weak impurity peaks indexed to $Li_xNi_{1-x}O$ are detected at the left shoulders of the (400) and (222) peaks. This is an ordinary occurrence, as this impurity originates from the Ni content, and the oxygen loss in samples annealed at high temperature reduces the amount of Ni in the spinel phase [2, 17, 18]. The intensity ratio of (4,0,0)/(3,1,1) increased as the temperatures rise, indicating presence of relatively extensive transition metal cation substitution in tetrahedral 8a sites of the spinel-type structure [19]. In previous research, Ohzuku et al. [20] have pointed out the occupancy of the 8a tetrahedral lithium sites by substituent ions will lead to some unfavourable electrochemical characteristics. For the sample annealed at 750 °C, the (4,0,0)/(3,1,1) intensity ratio is only 0.69, which is much smaller than for the others (0.89 at 680 °C and 0.97 at 820 °C). In this regard, the sample annealed at 750 °C is expected to show the best performance.

N_2 adsorption-desorption studies were also performed to determine the specific surface area of the LNMO. The Brunauer-Emmett-Teller (BET) surface areas were found to be 19.1, 16.5,

and 5.5 m^2 g^{-1} for the samples annealed at 680 °C, 750 °C, and 820 °C, respectively. A further increase in the reaction temperature leads to a smaller surface area of the sample.

Typical scanning electron microscope (SEM) images of the samples are presented in Figure 2. Fig. 2a shows that the sample annealed at 680 °C was composed of big secondary particles with rough surface compared to other samples in this study. The higher magnification SEM image in Fig. 2d shows that the primary particle size is in the range of 50-150 nm. The secondary particle size of the sample annealed at 750 °C is with an average diameter of 5 μm (Fig 2b). The primary particle size is approximately 100 nm (Fig 2e). As shown in Fig. 2 (c, g), well-defined particles 200-300 nm in diameter could be obtained after annealing at 820 °C. Therefore, the sample annealed at lower temperature has a relatively smaller particle size, and the result is consistent with the above BET analysis.

3.2 Electrochemical characterization

Figure 3(a-c) compares the charge-discharge voltage profiles of the Li/LNMO cells for the three samples in EC/DEC electrolyte. Figure 3(d) shows charge-discharge curves for the sample annealed at 750 °C in RTIL electrolyte. It should be noted that the cells with conventional electrolyte exhibit potential fluctuation at potentials higher than 5 V vs. Li/Li^+ for the initial charge, which can be attributed to electrolyte oxidation. Initial charge-discharge capacities and coulombic efficiencies for all cells are summarized in Table 1. The cells containing RTIL showed comparable discharge capacities and much higher coulombic efficiency compared to the conventional organic electrolyte. The extra charge consumption in the charging (oxidation) period for the conventional electrolyte can be related to the electrolyte decomposition and concomitant film deposition. The cells were successfully cycled in following cycles, however, suggesting the formation of a fairly stable solid electrolyte interphase (SEI), which protects the electrolyte against further degradation [21,

22]. In contrast, the cell was successfully cycled in RTIL, indicating that the electrolyte decomposition and film deposition are not severe in RTIL electrolyte. For the sample annealed at 820 ˚C, the small plateau at 4.1 V is due to the Mn^{3+}/Mn^{4+} redox couple caused by excessively fast cooling and oxygen deficiency during cooling of the sample [2]. Indeed, X-ray diffraction of this sample shows the presence of the impurity $Li_xNi_{1-x}O$ phase. The main charge plateau at 4.7 V is attributed to the Ni^{2+}/Ni^{4+} redox couple [23]. Furthermore, the potential corresponding to the transformation of Ni^{2+} to Ni^{4+} in the ionic-liquid-based electrolyte was lower than in the conventional electrolyte due to the lower ionic conductivity of RTIL at room temperature. This phenomenon has been observed in previous work on ionic-liquid-based electrolyte for lithium batteries [9, 10].

Figure 4 presents the coulombic efficiency of the samples in the different electrolytes. In general, coulombic efficiency steadily increased and then stabilized with cycle number. It is clear that the cells with RTIL electrolyte show much better performance than those with conventional electrolyte. The sample annealed at 750 °C shows the best coulombic efficiency among the three samples examined under the present experimental conditions. For conventional electrolyte, the average efficiency for the first fifteen cycles is 75.9 %. In contrast, the cell using RTIL has 88.6 % coulombic efficiency for the first fifteen cycles, which may be because the formation of a stable surface film on the electrode in RTIL is more favourable than in the conventional electrolyte [14]. This means that RTIL can improve the coulombic efficiency of LNMO. These features will be evidenced in the following electrochemical impedance spectroscopy (EIS) section.

Figure 5 shows discharge capacity versus cycle number for cells based on the different samples in different electrolytes. The sample annealed at 750 °C has the highest capacity. The capacities of LNMO with conventional electrolyte were higher than for samples with ionic liquid-based electrolyte. Similar performance has also been observed for $LiFePO_4$ [24]

and $LiCoO_2$ [25]. This can be explained by the dissolution of $[Li^+]$ $[NTf_2^-]$ salt in the $[C_4mpyr^+]$ $[NTf_2^-]$ ionic liquid, leading to a ternary system $[Li^+]_m[C_4mpyr^+]_n[NTf_2^-]_{(m+n)}$ with increased viscosity and lower conductivity, at the level of 1-2 mS cm^{-1} [26, 27]. The highly viscous electrolyte causes an increase in both electrolyte resistance and charge transfer resistance at the electrode/electrolyte interface. It leads to poor impregnation of the electrodes as well [28].

In order to gain further understanding of the differences in the electrochemical performance between the conventional and the ionic liquid electrolytes, the sample annealed at 750 °C, which had the highest capacity, was selected for EIS testing in different electrolytes. Before the EIS measurements, all the samples were charged to various potentials and maintained at charged potentials of 4.7 V and 5.1 V for 2 h. Fig. 6 shows the EIS results for lithium cells in the charged state at the 1^{st} and 6^{th} cycles. The impedance spectra reflect several processes that take place in series: Li migration through surface films, charge transfer, solid-state diffusion, and finally, accumulation of Li in the bulk of the active mass. According to previous impedance spectroscopy studies, the resistance associated with the higher frequency semicircle (typically, 300 Hz < f), R_{film}, is assigned to lithium-ion diffusion through surface films, and the charge-transfer resistance associated with the lower-frequency semicircle (typically, 0.1 Hz < f < 10 Hz), R_{ct}, is related to Li ion transportation across the surface film active mass interface [29]. Their values calculated from the diameters of the high-frequency and the medium-to-low frequency semicircles in the Nyquist plots for the electrodes are summarized in the Table 2. In general, the interfacial resistance continuously increased with the potential, which can be attributed to the formation of passive layer due to the reactivity of the lithium electrode and the electrolyte. It should be noted that the results obtained using RTIL electrolytes at 4.7 V are completely different from others. The impedance curves show one compressed semicircle related to the greatest frequency range of interest (high to low

frequencies) instead of separation of the different features. It means the electrode with RTIL is stable enough and R_f is low at the high frequencies, then the Nyquist plot becomes a steep line. The higher R_f is observed in the cell assembled with conventional electrolyte, while the cell assembled with RTIL has small value of R_f. As mentioned previously, it is because the RTIL leads to the formation of a stable SEI that protects against a further reductive decomposition of the electrolyte on the electrode, which permits the reversible migration of Li^+ ions through SEI. On the other hand, the charge-transfer resistance (R_{ct}) in RTIL is higher than that in conventional electrolyte for its highly viscosity. Furthermore, it has been reported that in the $LiPF_6$ solution LiF is a major constituent on the electrode surface, due to the reaction of the active surface with trace HF, which is unavoidably present [30]. Whenever LiF films are formed on the electrodes, their impedance becomes very high because of the high resistivity of LiF films so far as Li ion transport is concerned [31]. Accordingly, the cell assembled with the conventional electrolyte is shown to have much higher overall resistance than the cell with RTIL. After 5 cycles, it should be noted that the impedance in both types of electrolyte is reduced due to the stabilized SEI layer on the electrode surface.

4. Conclusions:

In summary, $LiNi_{0.5}Mn_{1.5}O_4$ nanoparticles can be prepared by a rheological phase method. RTIL ($C_4mpyrNTf_2$) can be a better electrolyte than the conventional alternative for $LiNi_{0.5}Mn_{1.5}O_4$ electrodes, as it improves the coulombic efficiency. The cell using RTIL as electrolyte shows a higher initial coulombic efficiency of 66.4%, while the cell using conventional electrolyte only shows an initial coulombic efficiency of 45.7 %. The results suggest that RTIL could be a promising electrolyte for $LiNi_{0.5}Mn_{1.5}O_4$ cells in terms of non-flammability, safety, and better electrochemical performance.

Acknowledgments: Financial support provided by the Australian Research Council (ARC) through DP110103909 and ARC Centre of Excellence funding (CE0561616) is gratefully acknowledged. The authors also want to thank Dr. T. Silver for critical reading of the manuscript.

References:

[1] T. Ohzuku, S. Takeda, M. Iwanaga, J. Power Sources, 81 (1999) 90.

[2] Q. Zhong, A. Bonakdarpour, M. Zhang, Y. Gao, J. R. Dahn, J. Electrochem. Soc., 144 (1997) 205.

[3] K. Ariyoshi, Y. Iwakoshi, N. Nakayama, T. Ohzuku, J. Electrochem. Soc., 151 (2004) A296.

[4] J. B. Goodenough, Y. Kim, Chem. Mater. 22 (2010) 587.

[5] J. S. Wilkes, M. J. Zaworotko, J. Chemical Soc. Chem. Comm., 13 (1992) 965.

[6] M. Galiński, A. Lewandowski, I. Stępniak, Electrochim. Acta, 51 (2006) 5567.

[7] M. Armand, F. Endres, D. R. MacFarlane, H. Ohno, B. Scrosati,. Nat Mater, 8 (2009) 621.

[8] N. Byrne, P. C. Howlett, D. R. MacFarlane, M. Forsyth, Adv. Mat., 17 (2005) 2497.

[9] J. Wang, S. Y. Chew, Z. W. Zhao, S. Ashraf, D. Wexler, J. Chen, S. H. Ng, S. L. Chou, H. K. Liu, Carbon, 46 (2008) 229.

[10] L. X. Yuan, J. K. Feng, X. P. Ai, Y. L. Cao, S. L. Chen, H. X. Yang, Electrochem. Comm., 8 (2006) 610.

[11] J. Z. Wang, S. L. Chou, S. Y. Chew, J. Z. Sun, M. Forsyth, D. R. MacFarlane, H. K. Liu, Solid State Ionics, 179 (2008) 2379.

[12] S. L. Chou, J. Z. Wang, J. Z. Sun, D. Wexler, M. Forsyth, H. K. Liu, D. R. MacFarlane, S. X. Dou, Chemistry of Materials, 20 (2008) 7044.

[13] S. Y. Chew , J. Sun, J. Wang, H. Liu, M. Forsyth, D. R. MacFarlane, Electrochim. Acta, 53 (2008) 6460.

[14] J. Mun, T. Yim, K. Park, J. H. Ryu, Y. G. Kim, S. M. Oh, J. Electrochem. Soc., 158 (2011) A453.

[15] D. R. MacFarlane, P. Meakin, J. Sun, N. Amini, M. Forsyth, J. Physical Chemistry B, 103 (1999) 4164.

[16] P. C. Howlett, D. R. MacFarlane, A. F. Hollenkamp, Electrochemical and Solid State Letters, 7 (2004) A97.

[17] M. Kunduraci, G. G. Amatucci, J. Power Sources, 165 (2007) 359.

[18] J. Cabana, S. H. Kang, C. S. Johnson, M. M. Thackeray, C. P. Grey, J. Electrochem. Soc., 156 (2009) A730..

[19] H. Wang, H. Xia, M. O. Lai, L. Lu, Electrochem. Comm., 11 (2009) 1539-1542.

[20] T. Ohzuku, K. Ariyoshi, S. Takeda, Y. Sakai, Electrochim. Acta, 46 (2001) 2327.

[21] P. C. Howlett, N. Brack, A. F. Hollenkamp, M. Forsyth, D. R. MacFarlane, J. Electrochem. Soc., 153 (2006) A595.

[22] P. C. Howlett, E. I. Izgorodina, M. Forsyth, D. R. MacFarlane, Zeitschrift für Physikalische Chemie, 220 (2006) 1483.

[23] S. B. Park, W. S. Eom, W. I. Cho, H. Jang, J. Power Sources, 159 (2006) 679

[24] S. Fang, Z. Zhang, Y. Jin, L. Yang, S. Hirano, K. Tachibana, S. Katayama, J. Power Sources, 196 (2011) 5637.

[25] H. Sakaebe, H. Matsumoto, K. Tatsumi, Electrochim. Acta, 53 (2007) 1048.

[26] C. A. Vincent, ed. Modern Batteries. Wiley. 1997.

[27] A. Fernicola, F. Croce, B. Scrosati, T. Watanabe, H. Ohno, J. Power Sources, 174 (2007) 342.

[28] K. Hayashi, Y. Nemoto, K. Akuto, Y. Sakurai, J. Power Sources, 146 (2005) 689.

[29] A. Zaban, E. Zinigrad, D. Aurbach, The Journal of Physical Chemistry, 100 (1996) 3089.

[30] D. Aurbach, I. Weissman, A. Zaban, O. Chusid, Electrochim. Acta, 39 (1994) 51.

[31] D. Aurbach, B. Markovsky, A. Shechter, Y. EinEli, H. Cohen, J. Electrochem. Soc., 143 (1996) 3809.

Figure Captions

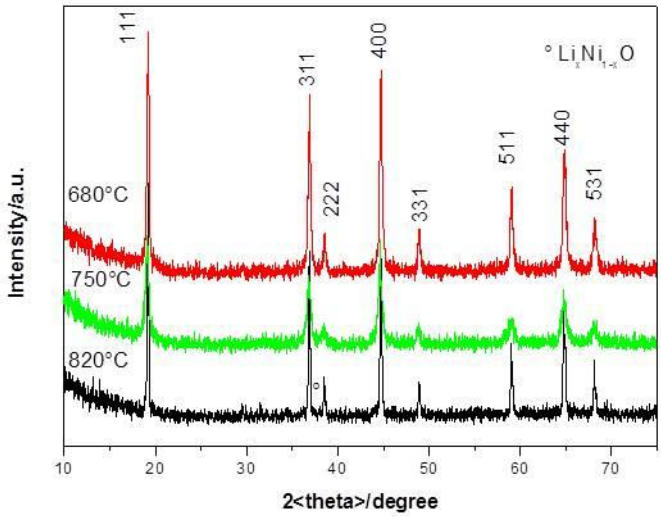

Figure 1. XRD patterns of the samples annealed at different temperatures: 680 °C, 750°C, and 820°C. (° indicates impurities.)

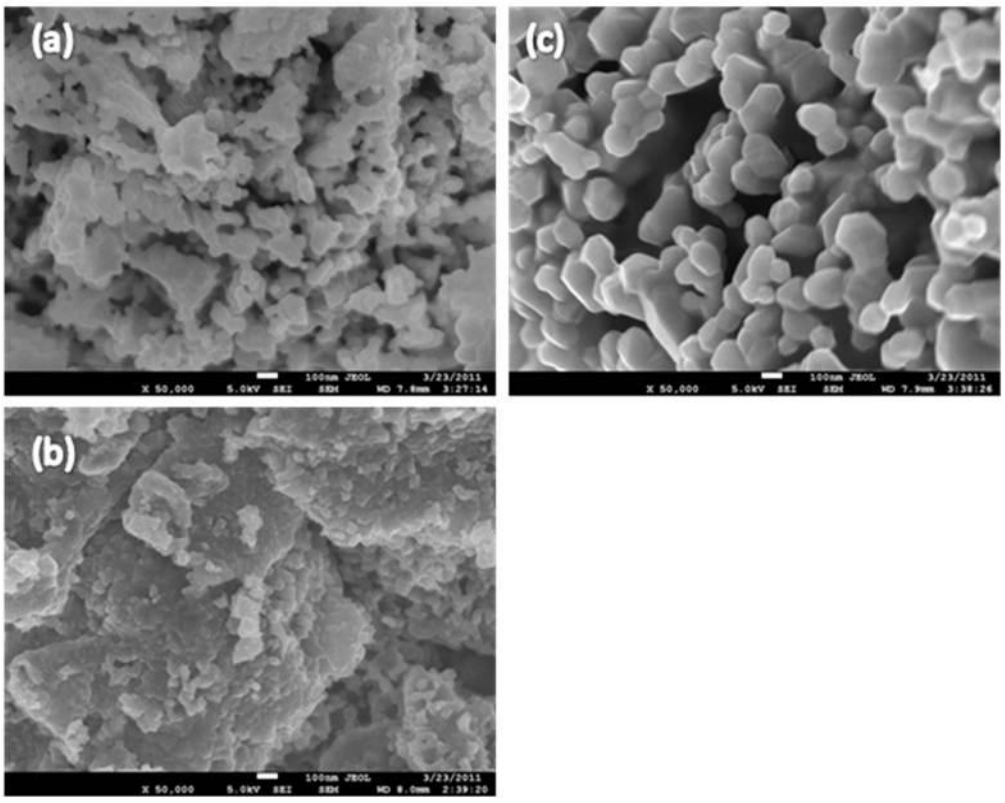

Figure 2. SEM images of samples annealed at different temperatures: 680 °C (a, d), 750 °C (b, f), and 820 °C (c, g).

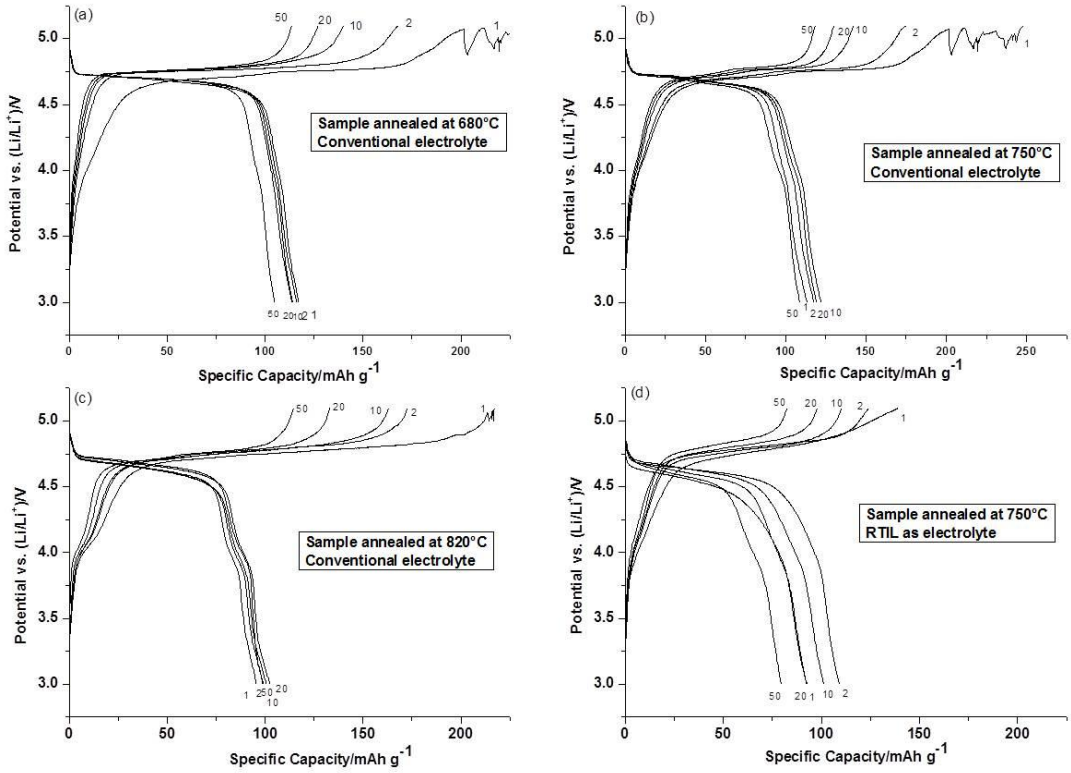

Figure 3. Charge-discharge curves for selected cycles for $LiNi_{0.5}Mn_{1.5}O_4$ electrodes made from samples sintered at different temperatures and used with conventional electrolyte or RTIL electrolyte.

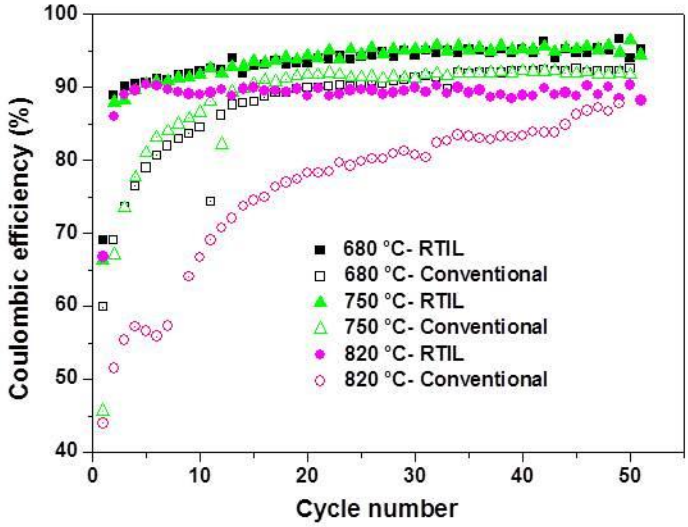

Figure 4. Coulombic efficiency of $LiNi_{0.5}Mn_{1.5}O_4$ electrodes with conventional and RTIL electrolytes.

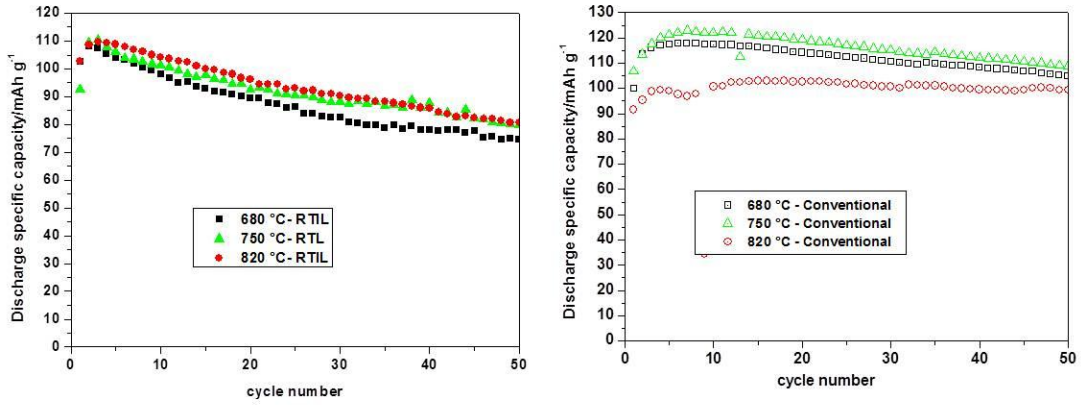

Figure 5. Cycle life of $LiNi_{0.5}Mn_{1.5}O_4$ annealed at different temperatures: (a) with RTIL electrolyte and (b) with conventional electrolyte.

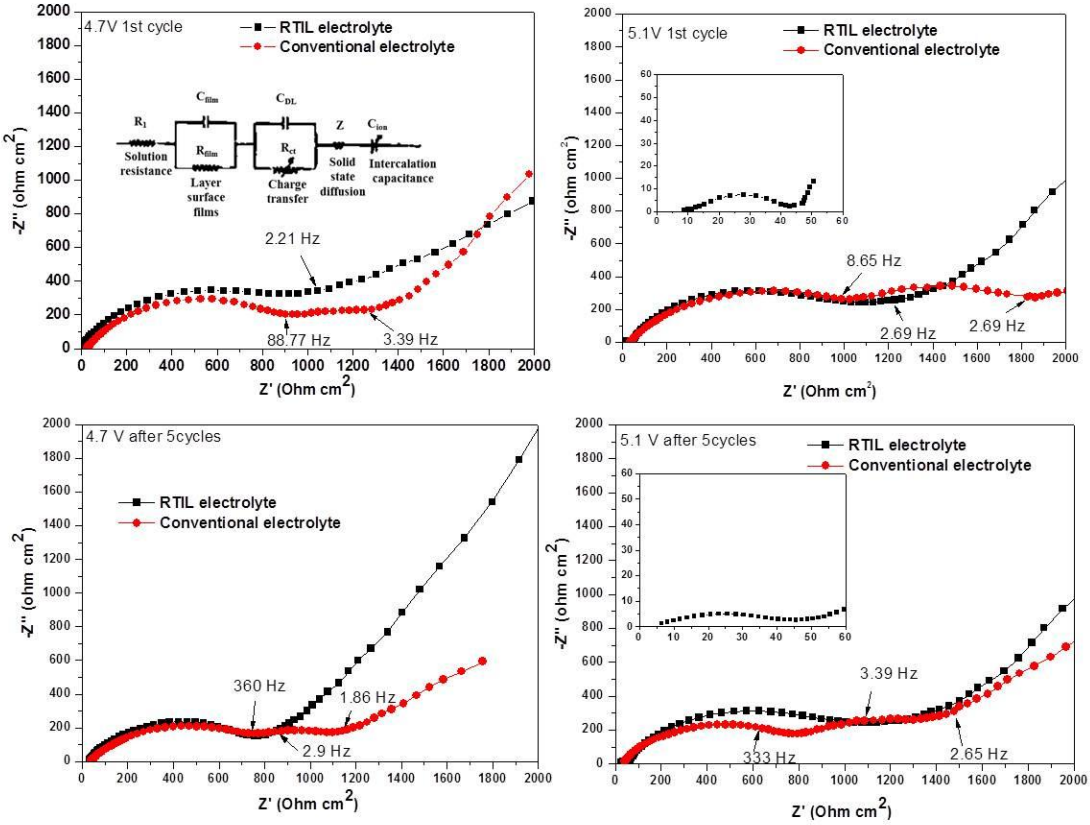

Figure 6 EIS spectra obtained from Li/ $LiNi_{0.5}Mn_{1.5}O_4$ cells for the 1st (top) and 6th (bottom) cycles using conventional and RTIL electrolytes. The electrode potentials are 4.7 V (left) and 5.1 V (right).

Table 1. Initial charge-discharge capacities and coulombic efficiencies.

Electrolyte	Capacity (mAh)		Coulombic efficiency (%)
	Charge	Discharge	
680 °C- Conventional	189.7	98.8	52.1
750 °C- Conventional	248.2	109.1	45.1
820 °C- Conventional	216.7	94.4	43.6
680 °C- RTIL	149.6	100.4	67.1
750 °C- RTIL	139.2	92.4	66.4
820 °C- RTIL	154.0	102.4	66.5

Table 2. R_{film} and R_{ct} for different testing states calculated from Nyquist plots for $LiNi_{0.5}Mn_{1.5}O_4$ spinel electrodes in different electrolytes.

	Conventional Electrolyte		RTIL	
Testing state	R_{film} (ohm cm^2)	R_{ct} (ohm cm^2)	R_{film} (ohm cm^2)	R_{ct} (ohm cm^2)
1st 4.7 V	1003	597	-	1310
1st 5.1 V	1208	1180	47	1143
6th 4.7 V	897	554	-	773
6th 5.1 V	990	1071	52	1311